2018

Full 3D numerical analysis of a roots blower with open-source software

Nicola Casari
University of Ferrara, Italy, nicola.casari@unife.it

Michele Pinelli
University of Ferrara, michele.pinelli@unife.it

Alessio Suman
University of Ferrara, alessio.suman@unife.it

Ahmed Kovacevic
a.kovacevic@city.ac.uk

Sham Ramchandra Rane
Centre for Compressor Technology, City University London, United Kingdom, sham.rane@city.ac.uk

See next page for additional authors

Full 3D numerical analysis of a roots blower with open-source software

Nicola CASARI[1]*, Michele PINELLI[1], Alessio SUMAN[1], Ahmed KOVACEVIC[2], Sham RANE[2], Davide ZIVIANI[3]

[1]University of Ferrara, Department of Engineering,
Via Saragat 1, 44122 Ferrara (FE) – ITALY
*nicola.casari@unife.it, michele.pinelli@unife.it , alessio.suman@unife.it

[2]City, University of London, Department of Engineering,
Northampton Square, EC1V 0HB, London, UK
A.Kovacevic@city.ac.uk , Sham.Rane@city.ac.uk

[3]Davide Ziviani, Purdue University, Ray W. Herrick Laboratories,
177 S Russell Street, West Lafayette, IN, 47907-2099, USA
dziviani@purdue.edu

* Corresponding author

ABSTRACT

In recent years, computational fluid dynamics (CFD) has been applied for the design and analysis of positive displacement machines (both compressors and expanders) for vapor compression and power generation (e.g., ORCs) applications.
The numerical modeling of the operation of such machines is challenging: the dynamics of the compression (or expansion) process and the deforming working chambers make the simulation process a not-trivial task. The relative motion of the rotors and the variation of the gaps during machine operation are few of the major challenges towards the implementation of reliable CFD models. Furthermore, the elaborated working fluid (i.e. the refrigerant) operates in many cases either close to the critical point or to the saturated-vapor line. Under such conditions, the ideal gas model does not hold and, thus, a compressible real gas solver is required.
Among the several numerical techniques that have been developed throughout the years, the custom predefined mesh generation is one of the most used techniques. In such an approach, a set of meshes is generated in advance before running the CFD simulation. The solver is fed with the mesh for each time step retaining the configuration of the mesh unchanged. In this work, SCORG-V5.2.2 was used to generate the meshes of the deforming domain around rotating parts of the machines. This was interconnected with OpenFOAM-v1606+, which is used to compute the flow field associated with the operation of the two-lobe Roots blower. It was demonstrated that the proposed methodology allows for a fast simulation and to achieve a good agreement with experimental test results.

1. INTRODUCTION

Positive displacement (PD) machines have a wide range of applications in modern engineering practice. Specifically, such machines have been employed as either compressor or expander in vapor compressor and power generation (e.g. ORCs). Among the several type of PD machines available, Roots blower has a long list of applications, as reported by (Blekhman *et al.*, 2004). Such machine is particularly appreciated for its high reliability, simplicity of design, predictable power consumption and large volumetric throughput. These features enabled this kind of machine to be widely employed in chemical and steel-making industries. Particularly, pneumatic conveying is one of the main application in which this machine is used.
Essentially, two different configurations are available for this device differing for the number of lobes. Two-lobe Roots blower are preferred for very high flow rate applications, whereas three-lobe type is appreciated for the lower pulsation level and less back-flow. This in turns implies reduced vibration and noise. This work deals with a two-lobe machine.

Over last years, Computational Fluid Dynamics (CFD) analysis (Casari *et al.*, 2017; Chang *et al.*, 2014; Kovacevic *et al.*, 2007; Morini *et al.*, 2015) has been regarded as a useful tool for the prediction of flow behavior and performance for PD machines, even though few contributions have been proposed concerning Roots blowers, e.g. Joshi *et al.*, (2006) The geometry complexity and the compatibility of the instrumentation make the experimental campaign very challenging. Sometimes the numerical approach is the only way to investigate the potential behavior of the machine with new fluids without major changes to the plant to be carried out. It must be remarked though, that such kind of numerical studies are very complicate. The complexity of the simulation has brought about the application of several numerical strategies to solve the volumetric machinery behavior. Among the other difficulties, the high mesh deformation asks for extra care during the mesh generation and motion evolution phases.

Several different approaches for tackling the problem are reported, for example, by (Casari *et al.*, 2017). In such work, different strategies for solving such issues are reported when solving the flow field on an unstructured mesh. Particularly, the Key Frame Remeshing (KFR) algorithm and the Mesh Adaption - Dynamic Remeshing are presented. The main idea is that most of the dynamic mesh solvers smooth the pre-defined boundary displacement inside the domain in such a way that the internal mesh is the solution of the boundary motion. The mesh is recomputed (globally or locally, according to the strategy chosen) if the cell quality falls below a certain threshold. A different approach is considered if one makes use of the overset grids, as reported for example by (Suman *et al.* 2017), or of the immersed boundary method, see Mittal & Iaccarino, 2005. In the first case, the mesh deformation is not solved, and the domain motion is accounted for by defining different regions corresponding to different areas involved in the deformation. Such regions are rigidly displaced, passing from the actual time step to the next: the relative motion is accounted for by checking the overlapping cells. Fluxes between the two regions are exchanged only if a certain number of cells is overlapping. For what concerns the immersed boundary method, the motion is considered by modifying the source term in the flow equations.

All the above-mentioned methods suffer from major drawbacks. Remeshing-based motion solvers are generally time-consuming and can easily lead to continuity errors, as suggested by Rane *et al.* 2013. Overset approach suffers of the same problem. IBM is poor in solving the boundary layer region, due to the non-aligned edges with respect to the wall.

An alternative approach is represented by the employment of body-fitted structured grids. Such meshes are easily stretched without losing quality, allowing for simulating the PD machine operation without need for remeshing, if the motion is properly solved. The mass conservation is not an issue any longer, since no remapping nor remeshing occur. The alignment between wall and edge in the nearby of the wall is always respected and the resolution of the flow close to the boundary is generally well resolved. Unfortunately, the definition of a structured grid compatible with the rotors displacement is not straightforward. Besides, the mesh motion should be somehow pre-defined in order to ensure the overall quality of the grid to be maintained over the evolution of the motion. If so called rotor to casing approach is used for discretization of boundaries, cells can collapse or deform to an invalid shape if the internal-node displacement is calculated by the dynamic motion solver.

The most favorable way to solve this is to use the custom predefined mesh generation: a set of meshes is prepared advanced, representing the control points through which mesh nodes pass. In such fashion, the mesh deformation is controlled. Pioneering work on development structured numerical meshes for rotary positive displacement machines have been reported by Kovacevic (2007). Grid generation is based on decomposition of the working domain using analytical transfinite interpolation and differential smoothing. This approach is now well accepted in industry and academia.

The custom predefined mesh generation algorithm is used in this work. SCORG-v5.2.2 with so called casing to rotor boundary discretization and conformal interface between the flow subdomains around the rotors was used for generating the set of meshes and OpenFOAM-v1606+ for the flow field solution. A new motion solver has been developed to force the mesh to pass through the control points.

2. METODOLOGY

The design condition of a two-lobe Roots blower has been numerically investigated in this work. In this section the numerical set-up and moving mesh algorithm are reported.

2.1 Mesh generation

In this paper, deforming grid of the twin screw machine is generated using algebraic transfinite interpolation and treated as an initial mesh upon which Elliptic PDE of the Poisson's form is solved. The resulting differential grid has highly improved cell quality and distribution. In addition, a special procedure has been introduced that completely

smooths the transition of the partitioning rack curve between the two rotors thus improving grid node movement and robustness of the CFD solver. A sample analysis of an oil injected twin screw compressor using the new Elliptic PDE grids has been presented (Rane *et al 2017*) to compare the improvements in grid quality factors in the regions of importance such as interlobe space, radial tip and core of the rotors. A significant improvement in the grid quality and robustness of numerical solver with higher order schemes has been obtained with this differential implementation of the deforming mesh. The overall size of the mesh is of roughly 500,000 cells: the pure hexahedral mesh in the rotor region is coupled with the cartesian mesh at the inlet and outlet ports. The mesh in the ports is obtained with the open-source software cfMesh (cross platform library for automatic mesh). The gap between rotor and casing is of 0.2 mm and the minimum clearance between rotors is 0.55 mm.

The Final mesh imported in OpenFOAM is the one reported in Figure 1. The quality of the grid produced is high, allowing to carry out the simulation without extra modification to the original mesh. For what concern the interface among the two lobes, an Arbitrary Mesh Interface (AMI) has been used. Such boundary type is required since the grid employed is non-confomal. The nodes on each side on the interface are thus non-coincident, demanding for a special treatment.

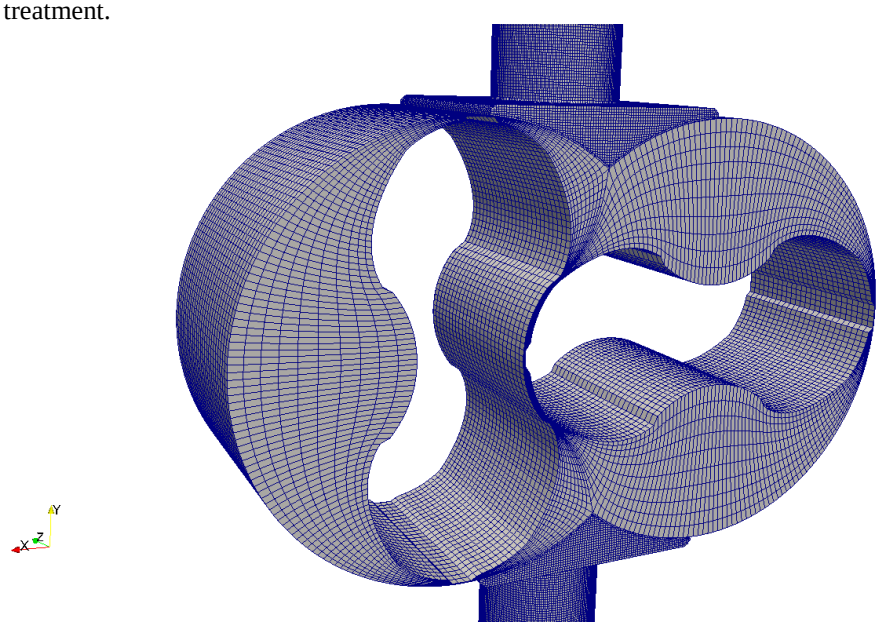

Figure 1 Mesh imported into OpenFOAM-Particular of the lobe area

2.2 Numerical set-up

The boundary conditions used in the numerical simulation are reported in Table 1. A pressure difference of 0.14 bar ha been imposed between inlet and outlet, with a rotational speed of 1800 rpm. Turbulence has been included as well, showing the computation is robust and can consider this important flow feature. The turbulence model used is a high-Re k-ε with standard wall functions.

The processed fluid is air and the conditions are such that the compressibility factor is close to the unity for in all the domain. Therefore, the ideal gas model has been used in this work. The simulation run fully parallel on 4 cores.

Table 1 Boundary conditions for the numerical simulation. No Gradient BCs are Neumann-type conditions

Quantity	Inlet	Outlet
Pressure [bar]	1.01	1.15
Temperature [K]	293	No Gradient
Velocity [m/s]	No Gradient	No Gradient
Turbulent kinetic energy	1 %	No Gradient

Turbulent kinetic energy dissipation rate	Mixing Length 0.0021 m	No Gradient

2.3 Mesh motion algorithm

The custom predefined mesh generation described in Par. 2.1 returns one grid file per degree. The developed library was at first implemented assigning to each node point its position at the next time step, by reading the actual and next grid file. This approach would make the time step assigned and equal to the time it takes to the rotors to span one degree. The simulations run with such time step were very unstable and it was indeed difficult to achieve convergence. In order to make the simulation more robust, the original algorithm was modified. Instead of assigning the time step, the user is left to choose the suitable time step for the computation, e.g. based on the maximum flux CFL desired. The actual position of the rotors and, consequently, of the entire grid is therefore computed by interpolation between two successive grids, as reported in Eqn. (1)

$$x_{i,final} = \alpha x_{i,AG} + (1-\alpha) x_{i,NG} \quad (1)$$

where $x_{i,final}$ represents the position of the node *i* at the actual time step, $x_{i,AG}$ is the position of the node *i* in the Actual Grid file, and $x_{i,NG}$ is the same for the Next Grid file. The Actual Grid and the Next Grid files are the output of the SCORG mesh generation process and contain the nodes location for the two instant we are interpolating among. The coefficient α is a blend factor function of the difference between the time step we are considering and the time interval between Actual Grid and Next Grid positions. The software handles the updating of the cell faces and volume automatically, since the variation of cell shape is provided as displacement. The new mesh metric is stored and employed for the next time step calculations.

2.4 CFD solution

To compute the machine performance, the *rhoPimpleDyMFoam* solver was employed. Such solver belongs to the set of compressible solvers that handle morphing meshes provided with OpenFOAM-v1606+. This solver uses the PIMPLE algorithm for the velocity- pressure coupling which, in turn makes use of the SIMPLE procedure (Patankar, 1980), including a number of PISO correctors (Issa, 1986). High Ma flows may make the solver unstable, and thus the convective terms of the pressure equation are treated implicit replacing the density values as a function of pressure. More details on its implementation can be found in (Gonzalez, 2016) The dynamic mesh library that can be handled by this solver is enriched with the new mesh motion algorithm proposed in section 2.3.

To close the motion problem, the equation of state is used to link the density to the pressure. In this work, the fluid processed by the machine is air in conditions close to the standard ones. Under such assumptions, it is reasonable to assume that the ideal gas law holds. Such model is therefore employed in this work.

3. RESULTS

The simulation run fully transient with a time step bounded by the maximum CFL = 0. 5. This condition translates in a time step roughly equal to 1e-6 s. The results of such analysis, under the conditions reported in the above section, are presented in this section.

3.1 Overall performance

The parameters monitored over the simulation run are the mass flow rate and the torque provided by the rotors. These two parameters are representative of the machine operation.

Figure 2 reports the flow rate variation under the boundary conditions provided in Table 1. The first two cycles of the machine have not been reported. An average flow rate of -0.0019 kg/s has been found as outcome of the analysis. This means the machine is operating with reverse flow: it tries to push the flow from low to high pressure, but the rotational velocity is too low to manage to overcome such head.

Besides, it can be clearly seen that the flow rate value has ripples that can be as high as 0.01 kg/s and the flow may be positive for some degree of the rotation of the shaft. These variations are expected even in case of standard flow direction. Such pulsations of the flow rate may represent an issue for the on-field application. A more stable output is among the reason that push operators to choose three-lobed machines, as suggested by (Kang, 2012). What it should be noted here is the repeatability of the pattern that can be assumed to be periodic with very good approximation. Such periodicity is expected and represents a qualitative validation of the implementation.

A rippled trend can be found also in the evolution of the torque, as shown in Figure 3. The torque provided by each of the rotors is the same, shifted of 0.00833 s corresponding to 90°, in agreement with the expectations. The power input that should be provided by an external source can be easily evaluated as $P = T\,\omega$, where T is the torque and $\omega = 2\,\pi n/60$ is the rotational speed. The average power consumption is therefore 190 W, spanning from a minimum of 110 W to a maximum of 235 W.

3.2 Detailed fluid-dynamics

The pressure evolution over an entire revolution of the rotor is reported in Figure 4. Passing from a) to e) the rotation causes the pressure pattern to change dramatically: the evolution is very similar to what is expected for this kind of machine, as reported, among the others by (Kang, 2012). It is particularly clear that the motion of the blower is expressed through increasing pressure in the chamber trapped by two rotors.

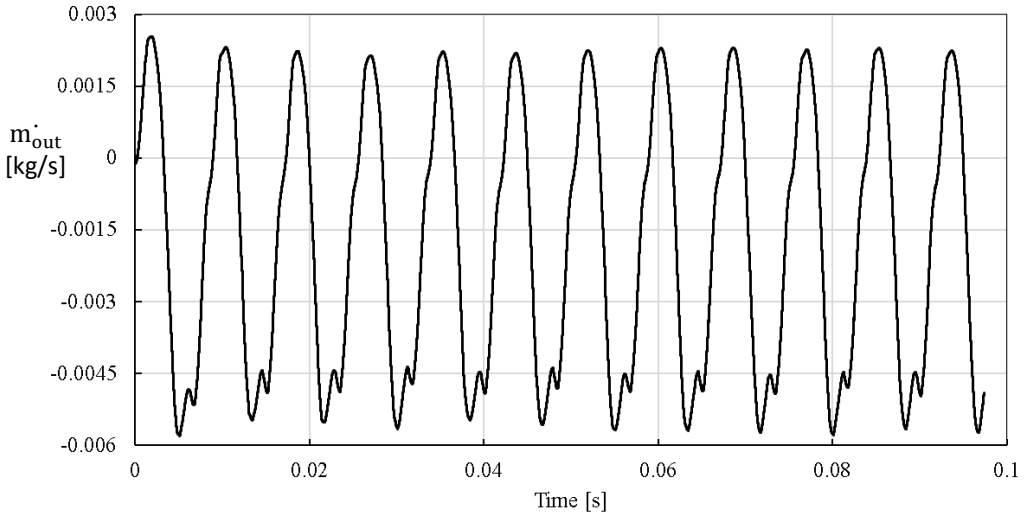

Figure 2 Mass flow rate measured at the outlet

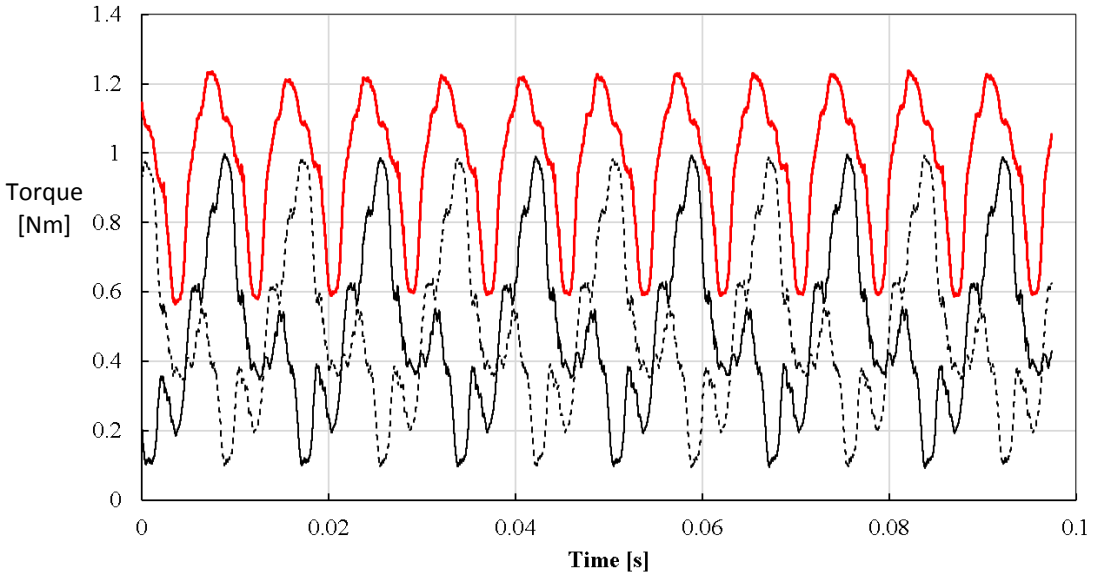

Figure 3 Torque on the two rotors and, in red, the sum

In this case the reverse flow acts retarding the discharge of the chamber, and this is particularly clear for example taking a look at Figure 4b). There, only the end of the lobe on the opposite side of the chamber with respect to the discharge port has a higher pressure with respect to the outlet domain and the flow is flowing from the outlet area inside the chamber, as if it was in the inlet area. This is particularly evident from the series of snapshots reported in Figure 5.

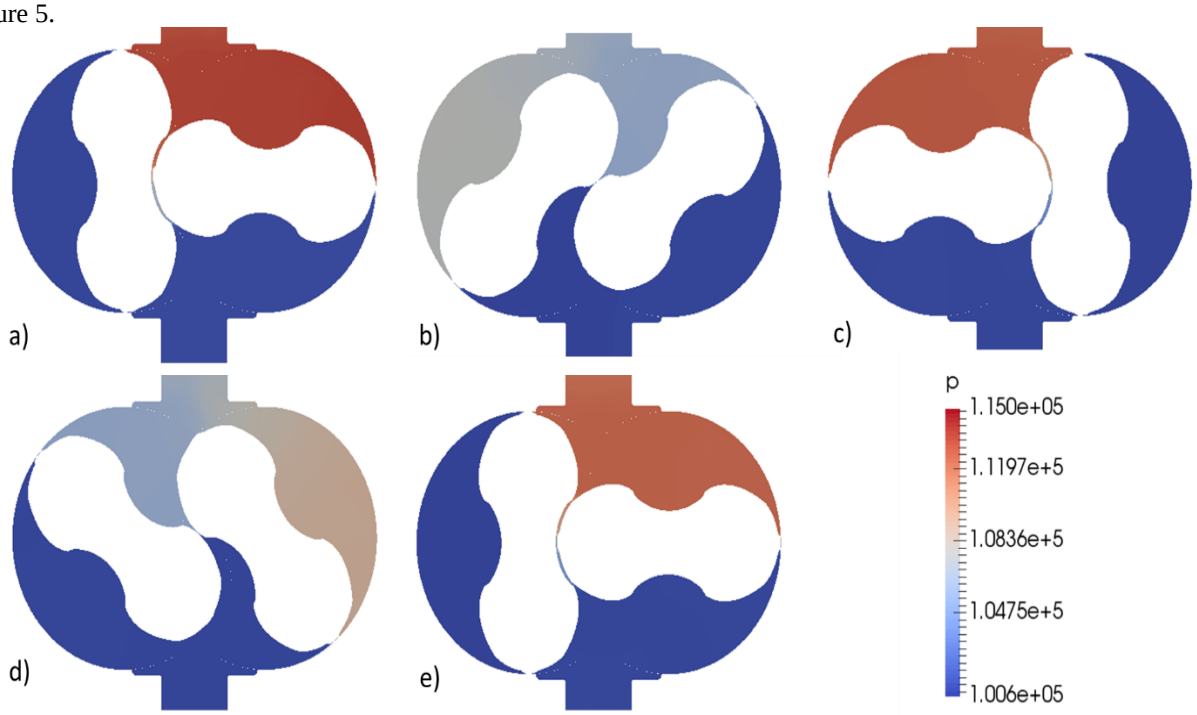

Figure 4 Evolution of the pressure over one half revolution of the rotor

With the implementation and the coupling carried out in this work, the complexity of all the fluid structures is correctly reproduced. One can, for example, look at Figure 5, where the opening chamber moment is reported. Starting from a), the lobe tip is approaching the outlet port opening. The fluid structures on the left hand side of the rotor are very irregular, due to the contemporary discharge phase of the left chamber and the flow coming back from the outlet. At the opening, b), the over-pressure discharge area tries to push the flow into the right chamber. This "backflow-jet" is detected for a small angular time, and in c) a new vortex forms, due to the rotor attempt to discharge the flow trapped inside the right chamber towards the outlet port/area.

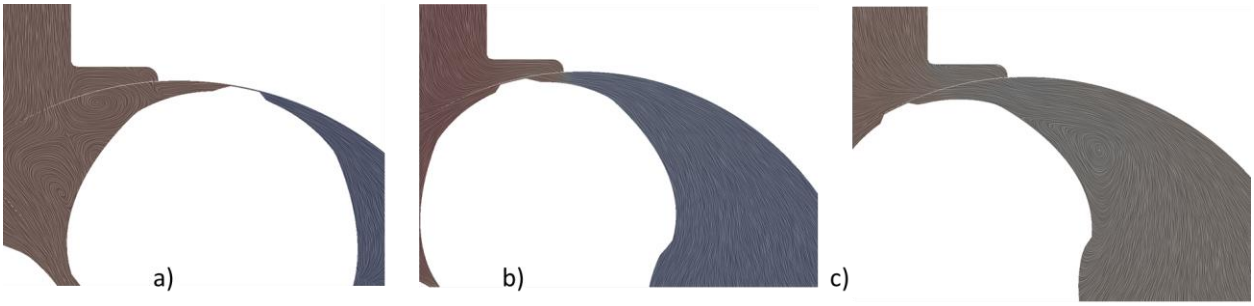

Figure 5 Vortex structures at the chamber opening

It may be of interest to see what happens in correspondence to the clearance among the two rotors. One can easily see that the usual structures in this area are correctly reproduced, showing no discontinuity in correspondence to the interface. The quite high velocities reached in the gap are handled without issues by the implementation presented in this work.

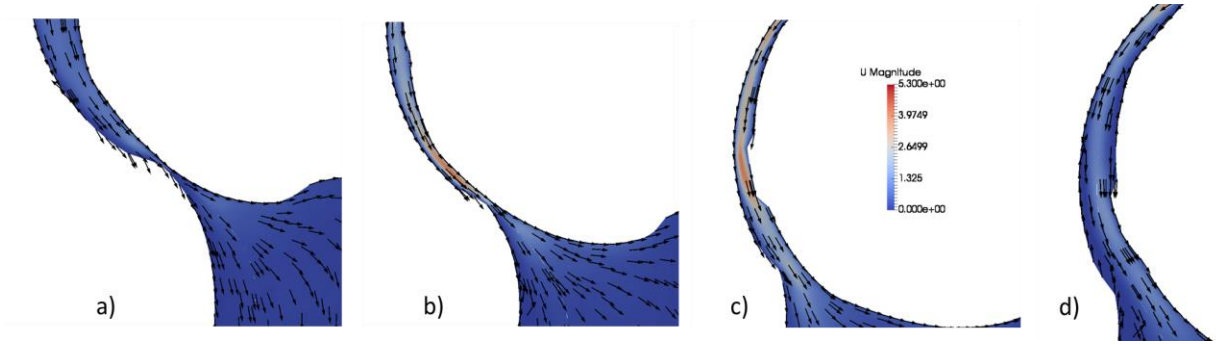

Figure 6 Flow field evolution in the clearance between the rotors

The simulation allows to observe features that are commonly of interest in the study of positive displacement machines. The gap between rotor and casing is one of the parameters that affects the machine performance the most, as well documented in the literature, for example by (Casari, 2017) and (Suman, 2017). Such gaps are, together with the clearance between rotors, the drivers of the volumetric efficiency of the machine. Figure 7 reports the velocity in the nearby of the gap, showing the evolution of the flow field in these important features. The 200 μm gaps are indeed a remarkable clearance for positive displacement machines and it can be clearly seen that a quite high amount of flow manages to escape from the chamber, lowering the volumetric efficiency of the machine. With the implementation carried out in this work, the complete pattern in the channel that forms due to the machine operation can be easily observed, as reported in the red box depicted in Figure 7.

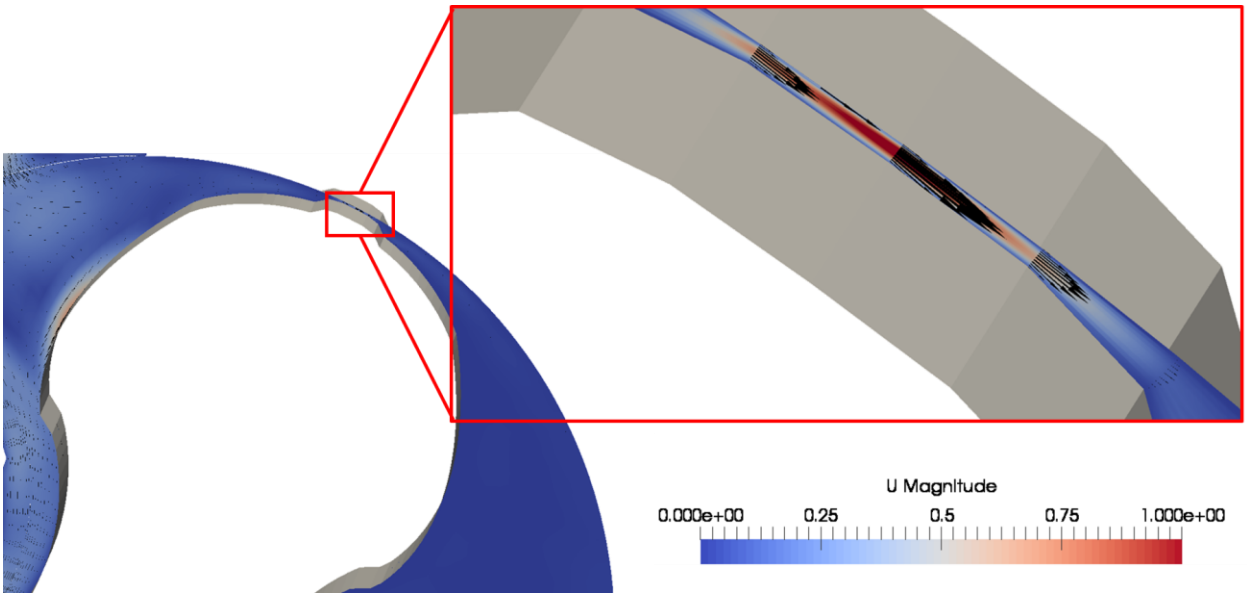

Figure 7 Rotor-Casing gap: flow field and velocity pattern

6. CONCLUSIONS

This work reports the numerical analysis of a positive displacement machine operating in reverse flow conditions. The simulation was carried out by OpenFOAM-v1606+ with the mesh provided by SCORG-v5.2.2. To move the mesh in such a way that it passes through the control points generated by the mesh generator, a new dynamic mesh library is implemented. Such library has been further improved since the fixed time step related to the position of the nodes was too unstable. A linear interpolation between two successive control points was implemented and the position of the node is automatically chosen in agreement with the time step. Such methodology was demonstrated to be robust, allowing to simulate particularly hostile condition, with reverse flow.
The main outcomes of this work are therefore:

- Development of a dynamic mesh library able to read the points generated from SCORG for driving the mesh. Such algorithm automatically blends between successive grids, allowing the user to choose the maximum time step allowable: the library takes care of the corresponding mesh motion;
- Simulation of a real positive displacement machine, having gap size that are close to the common engineering practice;
- The dynamic mesh approach used in this work allows to have stable and accurate simulations without need for remeshing: such procedure would involve the violation of the space conservation law, entailing the non-conservativeness of the mass.
- The procedure developed in this work is fully generalizable, able to simulate all the machines meshed with the casing-to-rotor technique from SCORG.

The validation of the results proposed here is considered a next step of this work.

NOMENCLATURE

CFL	Courant–Friedrichs–Lewy	(-)
$\dot{m}$	mass flow rate	(kg/s)
n	rotational speed	(rpm)
P	Mechanical Power	(W)
T	Torque	(Nm)
x	Node position	(m)

Greek symbols

α	blending factor	(-)
ω	rotational velocity	(rad/s)

Subscript

AG	Actual Grid file
Final	final position of the corresponding node
i	node index
NG	Next Grid file
out	outlet section
p	participants

ACKNOWLEDGEMENT

The research was partially supported by the Italian Ministry of Economic Development within the framework of the Program Agreement MSE-CNR “Micro co/tri generazione di Bioenergia Efficiente e Stabile (Mi-Best)”.

REFERENCES

Blekhman, D. I., Mollendorf, J. C., Felske, J. D., Lordi, J. A., & Joshi, A. M. (2004). Roots Compressor: High Temperature Testing and Modeling. In *ASME 2004 International Mechanical Engineering Congress and Exposition* (pp. 43–58). American Society of Mechanical Engineers.

Casari, N. Suman, A., Morini, M. & Pinelli, M. (2017). Real Gas Expansion with Dynamic Mesh in Common Positive Displacement Machines. *Energy Procedia*, 248--255.

Casari, N., Suman, A., Ziviani, D., van den Broek, M., De Paepe, M., & Pinelli, M. (2017). Computational Models for the Analysis of positive displacement machines: Real Gas and Dynamic Mesh. *Energy Procedia*, *129*, 411–418.

Chang, J.-C., Chang, C.-W., Hung, T.-C., Lin, J.-R., & Huang, K.-C. (2014). Experimental study and CFD approach for scroll type expander used in low-temperature organic Rankine cycle. *Applied Thermal Engineering*, *73*(2), 1444–1452.

Gonzalez, E. (2016). Cfd simulations of acoustic and thermoacoustic phenomena in internal flows. *46th AIAA Fluid Dynamics Conference*, (p. 3960).

Issa, R. I. (1986). Solution of the implicitly discretised fluid flow equations by operator-splitting. *Journal of computational physics*, 40-65.

Joshi, A. M., Blekhman, D. I., Felske, J. D., Lordi, J. A., & Mollendorf, J. C. (2006). Clearance analysis and leakage flow CFD model of a two-lobe multi-recompression heater. *International Journal of Rotating Machinery*, *2006*.

Kang, Y.-H. a.-H.-H. (2012). Factors impacting on performance of lobe pumps: A numerical evaluation. *Journal of Mechanics*, 229--238.

Kovacevic, A., Stosic, N., & Smith, I. (2007). *Screw compressors: three dimensional computational fluid dynamics and solid fluid interaction* (Vol. 46). Springer Science & Business Media.

Kovačević, A, Rane S. (2017). Algebraic generation of single domain computational grid for twin screw machines Part II – Validation, Advances in Engineering Software, 107, pp., doi: 10.1016/j.advengsoft.2017.03.001

Mittal, R., & Iaccarino, G. (2005). Immersed boundary methods. *Annu. Rev. Fluid Mech.*, *37*, 239–261.

Morini, M., Pavan, C., Pinelli, M., Romito, E., & Suman, A. (2015). Analysis of a scroll machine for micro ORC applications by means of a RE/CFD methodology. *Applied Thermal Engineering*, *80*, 132–140.

Patankar, S. (1980). *Numerical heat transfer and fluid flow*. CRC press.

Rane, S., Kovacevic, A., Stosic, N., & Kethidi, M. (2013). Grid deformation strategies for CFD analysis of screw compressors. *International Journal of Refrigeration*, *36*(7), 1883–1893.

Rane, S., Kovačević, A. (2017). Algebraic generation of single domain computational grid for twin screw machines. Part I. Implementation, Advances in Engineering Software, 107, pp. 38-50.

Suman, A., Randi, S., Casari, N., Pinelli, M., & Nespoli, L. (2017). Experimental and Numerical Characterization of an Oil-Free Scroll Expander. *Energy Procedia*, *129*, 403–410.